# Supporting Information

# Gate-Tunable High Magnetoresistance in Monolayer Fe$_3$GeTe$_2$ Spin Valves

Jie Yang,[1,2] Ruge Quhe,[5] Shiqi Liu,[1,2] Yuxuan Peng,[1,2] Xiaotian Sun,[6] Liang Zha,[1,2] Baochun Wu,[1,2] Bowen Shi,[1,2] Chen Yang,[1,2] Junjie Shi,[1,2] Guang Tian,[1,2] Changsheng Wang,[1,2] Jing Lu[1,3,4*] and Jinbo Yang[1,3,4*]

[1] State Key Laboratory for Mesoscopic Physics and School of Physics, Peking University, Beijing 100871, P. R. China

[2] Institute of Condensed Matter and Materials Physics, School of Physics, Peking University, Beijing 100871, P. R. China

[3] Collaborative Innovation Center of Quantum Matter, Beijing 100871, P. R. China

[4] Beijing Key Laboratory for Magnetoelectric Materials and Devices (BKL-MEMD), Peking University, Beijing 100871, P. R. China

[5] State Key Laboratory of Information Photonics and Optical Communications and School of Science, Beijing University of Posts and Telecommunications, Beijing 100876, P. R. China

[6] College of Chemistry and Chemical Engineering, and Henan Key Laboratory of Function-Oriented Porous Materials, Luoyang Normal University, Luoyang 471934, P. R. China

Email: jinglu@pku.edu.cn, jbyang@pku.edu.cn

**Table S1**. Monolayer $Fe_3GeTe_2$ spin valve performance with different split gate length and different gate spacing.

| $d$ (nm) | $L_g$ (nm) | $G_P$ (e²/h) | $G_{AP}$(e²/h) | MR (%) |
|---|---|---|---|---|
| | 1 | 3.59 | 0.60 | 495 |
| 0.11 | 2 | 3.35 | 0.71 | 374 |
| | 3 | 3.35 | 0.57 | 485 |
| | 1 | 3.32 | 0.71 | 369 |
| 1 | 2 | 3.37 | 0.69 | 390 |
| | 3 | 3.24 | 0.59 | 447 |

$d$ is the distance between two split gates. $L_g$ is the gate length of the split gate. $G_P$ and $G_{AP}$ are the conductance of the Fermi level in the parallel and antiparallel solutions.

**Table S2.** Magnetic moments of strain-induced ML $Fe_3GeTe_2$ with different methods ($m$, in $\mu_B$).

| | $m^{GGA+U}$ | $m^{GGA}$ | $m^{LDA}$ |
|---|---|---|---|
| −2% | 2.663 | 1.748 | 1.449 |
| −1.5% | 2.678 | 1.842 | 1.432 |
| −1% | 2.687 | 1.854 | 1.525 |
| −0.5% | 2.702 | 1.869 | 1.561 |
| 0% | 2.756 | 1.974 | 1.580 |
| | | | 1.484[a], 1.424[b], 1.625[c] |
| +0.5% | 2.742 | 1.976 | 1.623 |
| +1% | 2.765 | 1.998 | 1.682 |
| +1.5% | 2.794 | 2.013 | 1.738 |
| +2% | 2.818 | 2.026 | 1.792 |

[a, b] Previous calculation results of the averaged magnetic moment of the ML $Fe_3GeTe_2$. [1, 2]

[c] Experimental results of the magnetic moment of the bulk $Fe_3GeTe_2$. [3]
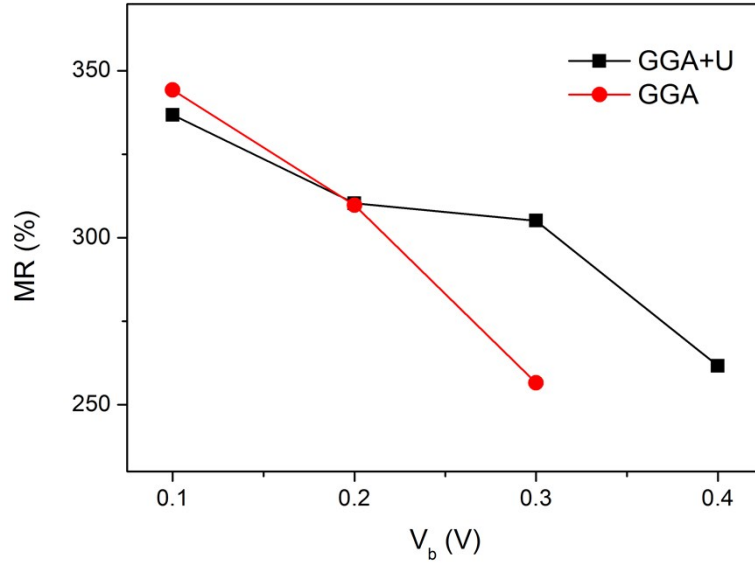
**Figure S1**. Magnetoresistance comparison of ML Fe$_3$GeTe$_2$ spin valve calculated with and without Hubbard $U$.

Zero equipotential lines are symmetrically distributed above and beneath the central region of the monolayer Fe$_3$GeTe$_2$ spin valve without gate. Noticeably, when adding the split gates, zero equipotential lines nearby the gates become flat and are different from the one without the gate. This different potential distribution caused by the existing gate makes the calculated MR vary though the boundary condition stays the same.
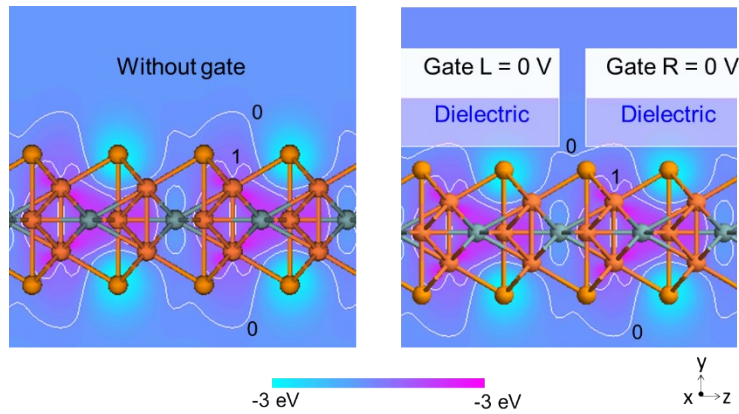


**Figure S2**. Hartree difference potential and equipotential lines before and after introducing spilt gate. The white lines represent the equipotential lines, given in eV.

Once both $G_P$ and $G_{AP}$ (or $I_P$ and $I_{AP}$) increase, how the MR changes is unsure because the MR will become either higher or lower. The MR strongly depends on the changing rate of $G_P$ and $G_{AP}$ ($I_P$ and $I_{AP}$). To summarize the gate effects on the MR, we plot the MR versus $\dfrac{a}{b}$, the ratio of the change rate of $I_P$ and $I_{AP}$, in the Figure 8. The relation between $\dfrac{a}{b}$ and the MR in the

top and bottom gate effected and split gates effected cases can be well fitted by MR$= 544.63 \times \dfrac{a}{b}$

$-100$ and MR$= 594.37 \times \dfrac{a}{b}$ $-100$, respectively. The slope of the linear functions is $\dfrac{I_\mathrm{P}}{I_\mathrm{ap}}$. The greater slope is, the larger conductance difference between two solutions. The greater slope appears in the split gates effected case, which is another fact that assures using split gate configuration can more efficiently boost the device MR.
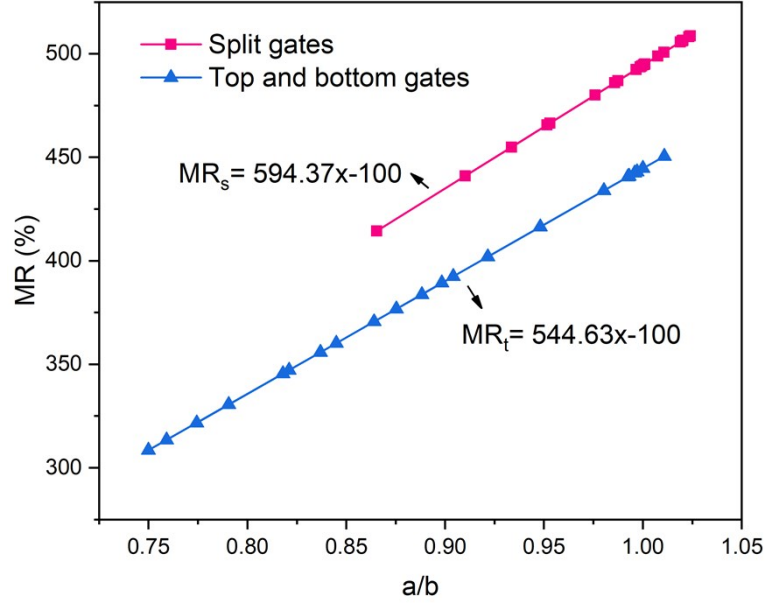


**Figure S3.** Magnetoresistance versus the ratio of the change rate of $I_\mathrm{P}$ and $I_\mathrm{AP}$ in the ML spin valve with top and bottom gates and split gates. The growth rates of $I_\mathrm{P}$ and $I_\mathrm{AP}$ are $a$ and $b$, respectively.

Stress effects, caused by lattice mismatch or deposition in the experiment, turn out inevitable and are known to have influences on magnetic properties. [4, 5] The homogeneous biaxial tensile and compressive forces along $x$ and $y$ directions ranging from $-2\%$ to $+2\%$ are applied to the ML $Fe_3GeTe_2$. The stability is evaluated by the cohesive energy difference between the strained and unstrained ML $Fe_3GeTe_2$ ($\delta E = E_\mathrm{strain} - E_\mathrm{unstrained}$). The strain makes the ML $Fe_3GeTe_2$ less stable because $\delta E$ is greater than zero (Figure S3 (a)). The ML $Fe_3GeTe_2$ with tensile forces within $+2\%$ is more stable than the composed ones. Besides, the strain changes the magnetic moment ($m$) of the ML $Fe_3GeTe_2$. $m$ of the unstrained ML $Fe_3GeTe_2$ is calculated as $2.756\mu_\mathrm{B}$. $m$ becomes $2.663\sim2.818\mu_\mathrm{B}$ as the strain is induced ($\varepsilon_{xy} = -2\% \sim +2\%$). The compressive (tensile) force reduces (increases) $m$ in comparison to the unstrained counterpart. We also compare the change of $m$ with the local density approximation (LDA) functional alone because in this method the obtained $m = 1.580\mu_\mathrm{B}$ is in agreement with the experimental result ($1.625\mu_\mathrm{B}$ for bulk $Fe_3GeTe_2$) and the previous theoretical prediction ($1.484\mu_\mathrm{B}$ [1] and $1.424\mu_\mathrm{B}$ [2] for the ML

Fe$_3$GeTe$_2$). After inducing the same range strain, $m$ becomes 1.432~1.792$\mu_B$ at LDA level, the same declining (increasing) tendency with the calculations at the GGA+$U$ level after inducing compressive (tensile) forces. All the calculations confirm the strain effects on $m$.

The detailed MR performance of the ML Fe$_3$GeTe$_2$ spin valve with mechanical stretch is also predicted. The $\varepsilon_{xy}$ = +0.5% stretched case is chosen. As Figure S3(b) shows, at small bias (0 < $V_b$ ⩽ 0.2 V), the MR increases under the strain effects. The maximum value reaches ~362% when $V_b$ = 0.2 V, basically equal to the unstrained maximum value (~392%). As $V_b$ continuously increases, the MR begins to decrease. The SFE is also taken into account, as shown in Figure S3 (c). The SFE of the stretched configuration ascends with the increasing $V_b$ for both the P and AP solutions. Compared with the unstrained device, the SFE of the stretched device in the P solution is greater under the same bias. The largest SFE of the stretched device in the P solution is over 40%, much higher than the unstrained maximum value (~10%). The SFE of the AP solution is also greater than that of the unstrained counterpart. The maximum SFE of the stretched device in the AP solution is over 50% when $V_b$ = 0.4 V, higher than the peak value of the unstrained case (~40%). The stretching intensifies the ability to produce current polarization of the ML Fe$_3$GeTe$_2$ spin valve because the greater $\alpha$ spin DOS of the stretched ML Fe$_3$GeTe$_2$ nearby the Fermi level (Figure S3) can drive more $\alpha$ spin electrons to get through under bias. With a stable level of the MR and a higher ability of the SFE, it is worth to expect that the ML Fe$_3$GeTe$_2$ with tensile force might open a route for manufacturing flexible spin-resolved devices.
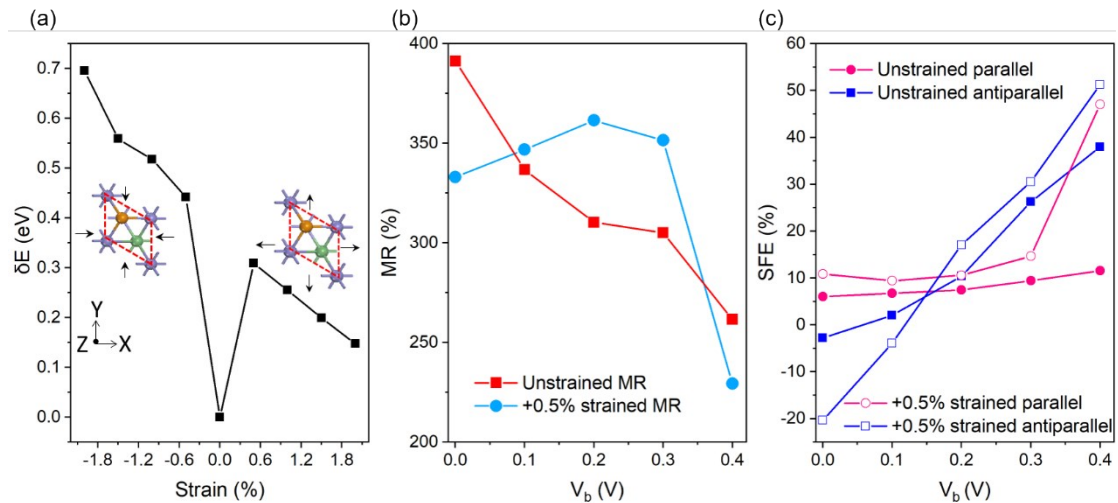


**Figure S4.** (a) Cohesive energy difference ($\delta E$) between strained and unstrained ML Fe$_3$GeTe$_2$ with $\varepsilon_{xy}$ = −2% ~ +2%. Black arrows in inset are the strain force directions. (b) Bias dependence of the magnetoresistance and (c) Comparison of the spin-filter efficiency of unstrained and

strained ML $Fe_3GeTe_2$ spin valve.
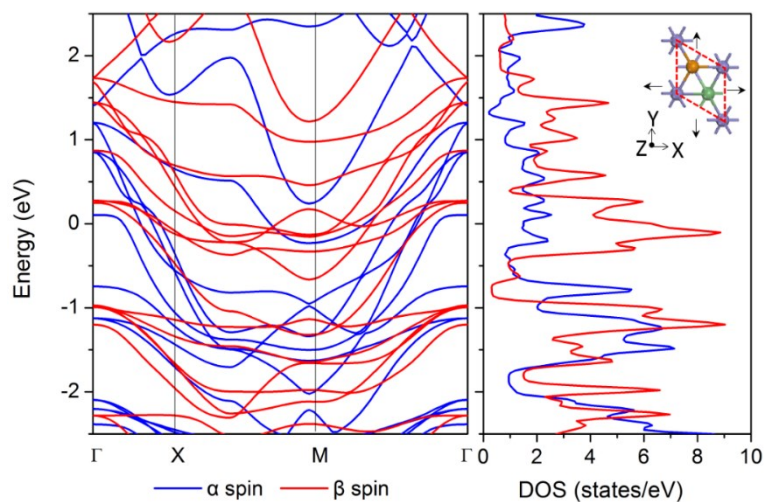


**Figure S5**. Spin-resolved band structure and density of states of $\varepsilon_{xy} = +0.5\%$ ML $Fe_3GeTe_2$.
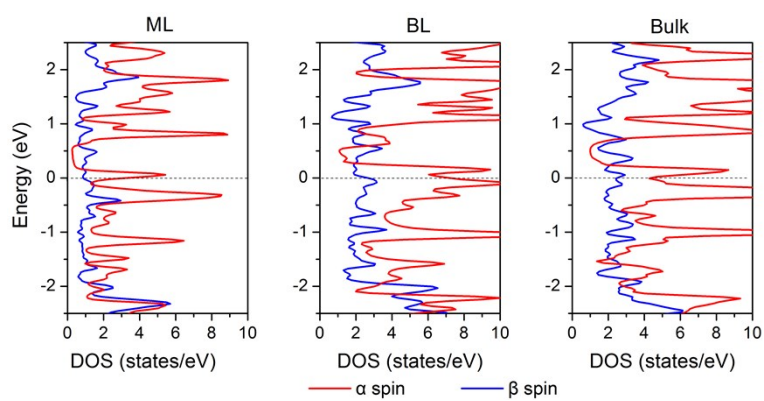


**Figure S6**. Spin-resolved density of states of monolayer, bilayer and bulk $Fe_3GeTe_2$. Fermi level is set to zero.

**References**

1.  Y. Deng, Y. Yu, Y. Song, J. Zhang, N. Z. Wang, Z. Sun, Y. Yi, Y. Z. Wu, S. Wu, J. Zhu, J. Wang, X. H. Chen and Y. Zhang, *Nature*, 2018, **563**, 94-99.

2.  H. L. Zhuang, P. R. C. Kent and R. G. Hennig, *Phys. Rev. B*, 2016, **93**, 134407.

3.  S. Das, H.-Y. Chen, A. V. Penumatcha and J. Appenzeller, *Nano. Lett.*, 2013, **13**, 100-105.

4.  S.-M. Choi, S.-H. Jhi and Y.-W. Son, *Nano Lett.*, 2010, **10**, 3486-3489.

5.  T. Hu and J. Dong, *Phys. Rev. B*, 2015, **92**, 064114.